Systematic Biology Advance Access published October 9, 2014

**Running head**

SHAPE EVOLUTION OF CERVICAL VERTEBRAE IN TURTLES

**Title**

Evolution of Neck Vertebral Shape and Neck Retraction at the Transition to Modern Turtles: an Integrated Geometric Morphometric Approach

**Authors**

Ingmar Werneburg[1,2,*], Laura A.B. Wilson[3,*], William C. H. Parr[4], Walter G. Joyce[5]

**Corresponding addresses**

1 - Paläntologisches Institut und Museum der Universität Zürich, Karl-Schmid-Strasse 4, 8006 Zürich, Switzerland

2 - Museum für Naturkunde, Leibniz-Institut für Evolutions- & Biodiversitätsforschung an der Humboldt-Universität zu Berlin, Invalidenstraße 43, 10115 Berlin, Germany

3 - School of Biological, Earth & Environmental Sciences, University of New South Wales, Kensington NSW 2052, Australia;

4 - Surgical and Orthopaedic Research Laboratories, Prince of Wales Clinical School, University of New South Wales, Randwick , NSW 2031, Australia

5 - Department of Geosciences, University of Fribourg, 1700 Fribourg, Switzerland

* corresponding author: i.werneburg@gmail.com

* corresponding author: laura.wilson@unsw.edu.au

**Abstract**

The unique ability of modern turtles to retract their head and neck into the shell through a side-necked (pleurodiran) or hidden-necked (cryptodiran) motion is thought to have evolved independently in crown turtles. The anatomical changes that led to the vertebral shapes of modern turtles, however, are still poorly understood. Here we present comprehensive geometric morphometric analyses that trace turtle vertebral evolution and reconstruct disparity across phylogeny. Disparity of vertebral shape was high at the dawn of turtle evolution and decreased after the modern groups evolved, reflecting a stabilization of morphotypes that correspond to the two retraction modes. Stem turtles, which had a very simple mode of retraction, the lateral head tuck, show increasing flexibility of the neck through evolution towards a pleurodiran-like morphotype. The latter was the precondition for evolving pleurodiran and cryptodiran vertebrae. There is no correlation between the construction of formed articulations in the cervical centra and neck mobility. An increasing mobility between vertebrae, associated with changes in vertebral shape, resulted in a more advanced ability to retract the neck. In this regard, we hypothesize that the lateral tucking retraction of stem turtles was not only the precondition for pleurodiran but also of cryptodiran retraction. For the former, a kink in the middle third of the neck needed to be acquired, whereas for the latter modification was necessary between the eighth cervical vertebra and first thoracic vertebra. Our paper highlights the utility of 3D shape data, analyzed in a phylogenetic framework, to examine the magnitude and mode of evolutionary modifications to vertebral morphology. By reconstructing and visualizing ancestral anatomical shapes we provide insight into the anatomical features underlying neck retraction mode, which is a salient component of extant turtle classification.

**Keywords**

Neck mobility, neck retraction, 3D warping, phylomorphospace, ancestral shape reconstruction, Pleurodira, Cryptodira, Testudines, Testudinata

Modern turtles are characterized by the ability to retract their neck and head inside the body wall (i.e., within their shell), but whereas cryptodiran turtles retract the neck in a vertical plane between the shoulder girdles (Fig. 1A), pleurodiran turtles retract their neck in a horizontal plane and place it anterior to the shoulder girdles (Fig. 1B). Given how prominently these neck retraction mechanisms feature in the classification of extant turtles, it is not surprising that paleontologists utilized this character complex to infer phylogenetic relationships. During the early half of the 19$^{th}$ century, fossil turtles were generally shoehorned into extant genera [summarized by (Maack 1869)], but following the Darwinian revolution, it became increasingly apparent that many fossil turtles represented extinct or ancestral lineages. Although materials were limited at the time, Lydekker (1889) referred most Cenozoic fossil material to Pleurodira or Cryptodira, but he also noticed that many older, mostly Mesozoic forms (Fig. S1A-D), are intermediate in morphology. He therefore classified these turtles separately as the "Amphichelydia*"* (lit. 'both-turtles') and diagnosed the group by a series of shell characters and the absence of formed articulations of the vertebral centra (i.e., centra that articulate along convex/concave joints). Paleontologists universally accepted this classificatory system for the next 100 years (Baur 1890, Hay 1908, Williams 1950, Romer 1956), although Simpson (1938) and Romer (1956) noted that the "Amphichelydia" likely represented an unnatural (paraphyletic) group. Following more than 30 years of cladistic methodology, it is now universally accepted that all characters that were used to define "Amphichelydia" actually represent plesiomorphies and that the two specialized neck retraction mechanisms evolved independently from one another within the turtle crown (Gaffney 1975, Gaffney 1996, Hirayama, Brinkman et al. 2000, Gaffney, Rich et al. 2007, Joyce 2007, Anquetin 2011, Sterli and de la Fuente 2013).

All turtles have eight cervical vertebrae (CV1 to CV8) (Fig. S1) (Williams 1950, Müller, Scheyer et al. 2010), which articulate along their vertebral centra ("central articulation") and their zygapophyses (see Fig. 2 for terminology). The last cervical articulates with the first vertebra of the body (dorsal vertebra one, DV1). Beyond our tentative assumption that a key change took place in the anatomy of cervical vertebra eight (CV8) to establish the retraction of the whole neck in modern turtles, all vertebrae along the cervical column must have undergone extensive morphological modifications to achieve a greater amount of internal mobility along the neck (Figs 1A-B, S1E-F). However, it is also possible that the unique relationship between CV8 and the body (DV1) did not require special morphological evolution, but rather resulted as a consequence of the cumulative change that occurred within the entire vertebral series.

The short and compact vertebrae and the absence of formed vertebral centra in most stem turtles have been use to argue that stem turtles lacked the ability to retract their heads and necks (e.g., (Gaffney 1990)). In a recent study, however, Werneburg et al. (in press) highlighted that stem turtles were likely able to retract their head and neck by laterally tucking them below the anterior edge of the shell (Fig. 1C), a trait acquired in parallel with the acquisition of their body armor. To achieve this movement, only slight internal rotation and ventral movement of adjacent vertebrae were needed and the shape of the vertebral centra only required little modification (Werneburg, Hinz et al. in press).

When studying vertebral evolution in turtles, it is a challenge to score discrete characters, because vertebrae are very similar between species, and because there exist significant differences in vertebral dimensions within the vertebral column (Fig. S1) that are best characterized by morphometric measures and evaluated by morphospace occupation. Williams (1950) nevertheless found characteristic vertebral formulae for the major groups of

extant turtles that were based on the shape of the central articulations only. Although he did not resolve the interrelationship of taxa in his pre-cladistic study, his classification foreshadows much of the current understanding of turtle taxonomy. However, whereas these descriptive formulae are useful in diagnosing many of the modern clades of turtles, they are less useful in resolving the relationships of fossil turtles lacking formed cervical centra (Joyce 2007).

In the present paper, we use a 3D geometric morphometric approach to investigate the evolution and phylogenetic signal of cervical vertebral shape across a broad sample of extinct and extant turtle species. We circumvent problems associated with the use of discrete characters by using landmark data. We test three major hypotheses.

Hypothesis 1 (*Evolution of Shape Change*): Given the extensive diversification at the dawn of modern turtle clades, we hypothesize a high level of shape disparity at the time when modern turtle diversification took place. We raise the question, whether subclade disparity is higher than expected under neutral evolution (Brownian motion) or whether there are temporal shifts in disparity values associated with subclade diversification.

Hypothesis 2 (*Cryptodira vs. Pleurodira*): Given the clear phylogenetic differentiation between Pleurodira and Cryptodira, we hypothesize that the ancestral vertebral shapes of both clades were strikingly different from the common ancestor of crown turtles (Testudines) and of all turtles (Testudinata, sensu (Joyce, Parham et al. 2004)). We ask what the ancestral state of vertebral shapes looked like and what the morphological transformations were that led to modern turtle morphotypes.

Hypothesis 3 (*Stem Turtle Retraction*): Given the short necks of stem turtles and the concave to flat articulation facets of their cervical centra, our null-hypothesis is that stem turtles were not able to retract their necks in the way that extant cryptodires and pleurodires do. We ask if

any specific shapes are apparent in the vertebral anatomy of modern turtles that can be directly related to modern neck retraction and if those features are absent in stem turtles.

## Materials and Methods

### *Specimens and 3D-Scans*

We studied the first to eighth cervical vertebrae (CV) of five extinct and 35 extant turtle species (Table S1-2). The surfaces of larger fossil and macerated neck vertebrae were scanned with a Next Engine 3D-scanner and reconstructed with ScanStudio HD Pro software (Anthropology Department Tübingen/Germany). Each vertebra was scanned horizontally and vertically with nine divisions within 360°. 10,000 points/inch$^2$ were taken ("CD quality") and each 360° scan required about ten minutes. Surface mesh-files were generated in ply-file-format.

Micro computed tomography (µCT) was performed for most macerated vertebrae at the Steinmann-Institut für Geologie, Mineralogie und Paläontologie at the Rheinische Friedrich-Wilhelms-Universität Bonn with a resolution of 187µm and at the Riedberg Campus of the Goethe-Universität Frankfurt with a resolution of 25 µm. Selected large fossil vertebrae (e.g., those of *Meiolania platyceps*) were CT-scanned with the medical CT-scanner at Universitätsklinikum Tübingen with a resolution of 600µm.

The data set was processed using the software program Amira 5.2.2 and surface meshes (obj- and ply-files) were generated with the same software.

### *3D-Geometric Morphometrics of Vertebral Shapes*

The surface mesh files were imported into the software program Landmark ver. 3.6 (Wiley, Amenta et al. 2005). In total, 25 landmarks were selected to represent clearly homologous

points (Figs 2, S2, Table S3). Prior to further analyses, landmark data were Procrustes superimposed to remove the effects of rotation, translation, and size (Rohlf 1990) using PAST ver. 2.16 (Hammer, Harper et al. 2001). Landmarks captured on all CVs were entered into an initial Principal Component Analysis (PCA). Eigenvalues, percent variance, centroid sizes and scores of PC-axes 1-7 were noted (Table S4-5). Trajectories of shape change between successive vertebrae (i.e., joining CV2 to CV3 to CV4, etc.) were drawn in PC1 vs. PC2 morphospace to provide a simple visual representation of shape change, these are here referred to as 'shape gradients' (Fig. 3). In order to study anterior and posterior vertebral shape separately, landmark clouds were halved and analyzed separately (Fig. S4, Table S6-7). The PC scores of each vertebra were plotted against the anterior plus the posterior angles measured for the raw mobility of particular vertebrae. Raw mobility refers to the maximum mobility mechanically allowed between two vertebrae. For that, the centra and the zygapophyses of adjacent vertebrae keep contact and the vertebrae are rotated in a plan orientation [see Werneburg et al. (in press) for further details]. PC-scores of the anterior and the PC-scores of the posterior facets of the vertebrae were plotted against the angles measured for each facet separately (Table S8). For that, the measurements of raw mobility of all adjacent vertebrae (Table S2) were plotted against PC scores (Table S8, Fig. S3).

***Phylogenetic Framework***

Although much progress has been made in the last decades, the phylogenetic relationships of many fossil and extant turtle clades are still controversial (Fig. S9). However, two primary viewpoints can be discerned with regard to the phylogenetic placement of fossil turtles (Joyce and Sterli 2012). On the one side, early cladistic analyses (Gaffney 1975, Gaffney and Meylan 1988) and some more recent numerical cladistic analyses (Hirayama, Brinkman et al. 2000, Gaffney, Rich et al. 2007) support the hypothesis that all known post-Triassic turtles

are placed within crown group Testudines. The vast majority of more recent, numerical cladistic analysis and combined analysis, on the other side, interpret a number of fossil taxa as stem turtles, including the Gondwanan clade Meiolaniidae and the predominantly North American clade Paracryptodira. We herein concentrate on this second hypothesis of fossil turtle interrelationship because it is based on more data (Figs 4, S7).

Given that there is no morphological agreement in regard to the arrangement of the extant groups of cryptodires (Fig. S9), we follow molecular topologies for crown cryptodires (Danilov and Parham 2008) as these are based on more data. *Indotestudo*/*Testudo* species were set as unresolved (Thomson and Shaffer 2010).

On a finer scale, the phylogenetic position of the fossil taxon *Naomichelys speciosa* (Fig. S1D) is not well resolved (Joyce, Sterli et al. in press), because it has only been included in two cladistic analyses that either favor the historical association of this taxon with Paracryptodira (Hirayama, Brinkman et al. 2000) or with Meiolaniidae (Anquetin 2012). Yet, inclusion of this taxon is of importance for this analysis because a well-preserved neck was available for our study. We therefore secondarily insert this taxon into the favored topology using the morphometric data obtained herein.

### *Time Calibrations*

To calibrate the topology used for phylomorphospace plots and disparity analyses (see below), we mainly rely on the data of Joyce et al. (2013), who calculated node age as part of a comprehensive fossil calibration study (Table S9).

### *Data composition for Phylogenetic Analyses*

We divided our landmark data set by vertebra to analyze CV2, CV5, and CV8 separately, chosen to provide insight into shape change occurring at the anterior, central and posterior

regions of the cervical column. These three data sets were used for phylomorphospace construction, disparity calculations and ancestral shape reconstruction.

For *Xinjiangchelys qiguensis*, we used the mean shape of the existing three, very similar vertebrae and set it as the mean shape for all vertebrae in that species, which resembles most of the actual condition. Although the vertebrae could not be identified, we included this taxon due to its important phylogenetic position along the stem of cryptodires. Taking the average shape was reasonable given the very similar position of vertebrae in morphospace and hence low magnitude of group variance (mean summed squared distance about mean value = 0.026) (Fig. S2E-G).

The atlas (CV1) was excluded because data on this vertebra was only available for five species and its shape is drastically different to those of the other neck vertebrae. Principal Component Analysis (PCA) was conducted separately for the CV2, CV5 and CV8 data sets, and the outputted scores were used for visualizing shape differences between species using phylomorphospaces, and for disparity analyses.

### *Ancestral Shape Reconstruction*

Using landmark data, we used squared-change parsimony (Maddison 1991) and reconstructed the ancestral landmark configuration of cervicals 2, 5, and 8 for of the last common ancestors of Testudinata, Testudines, Cryptodira, and Pleurodira. The selection of 3 out of 8 neck vertebrae was reasonable to get an estimation of shape change along the cervical column. Shape change in CV3-4 and CV6-7 are expected to align between the selected vertebrae. Major anatomical changes, moreover, are expected for CV5, one of the "kink-vertebrae" during pleurodiran retraction (Fig. 1B) and in CV8, which articulates with the trunk (Herrel, Van Damme et al. 2008).

For 3-dimensional shape visualization (Figs 5-7), we reconstructed the 3D morphology of the cervical vertebrae CV2, 5 and 8 of *Proganochelys quenstedti,* being at the base of the topological tree (Fig. 4), from CT-data. These cervical 3D reconstructions form the original surface mesh for warping. The Template Mesh Deformation (TMD) method was used to warp these original *P. quenstedti* surface meshes to target shapes of nodes 2 (Testudinata), 5 (Testudines), 7 (Cryptodira) and 34 (Pleurodira) on the tree (Gunz, Mitteroecker et al. 2009, Parr, Wroe et al. 2012). The target template shapes in this case are the calculated landmark positions at these ancestral nodes. The shape transformation between the original *P. quenstedti* landmark configuration and the target ancestral node landmark configuration was used as the basis for warping the 3D surface mesh of the *P. quenstedti* CVs (Parr et al., 2012). The resulting shapes were then Procrustes superimposed to minimize differences in orientation and size between the different comparisons in Figs 5-7 (Gower 1975, Rohlf and Slice 1990). Minimizing differences in orientation and size between warped 3D models, along with assigning each node model a different color and making the warped 3D models translucent, best highlights the differences in shape between the two vertebral models in each comparison. This was performed in Mathematica ver. 9.0 (http://www.wolfram.com/mathematica).

***Phylomorphospace Projections***

Phylomorphospaces were used to visualize the relationship between phylogeny and taxon spacing in shape space and infer evolutionary modes of shape change (Fig. 8). These were constructed using Principal Component (PC) scores outputted from separate PCAs conducted on the cervical vertebrae two, five, and eight data sets. Following Sidlauskas (2008), the Plot tree 2D algorithm in the Rhetenor module (Dyreson and Maddison 2003) of Mesquite (Maddison and Maddison 2011) was used to construct phylomorphospaces for PC1 vs. PC2,

capturing the maximum shape variance and also PC1 vs. PC3 and PC2 vs. PC3 (see supplementary files). The Rhetenor module reconstructs the ancestral states along PC axes, plots all terminal and internal nodes into the morphospace defined by those axes and then connects adjacent nodes by drawing branches between them. Subsequent axes (i.e. PC4, PC5) were not plotted as they were not deemed significant under the broken-stick model (Jackson 1993).

For CV2, CV5 and CV8, Procrustes distances were computed between ancestral landmark configurations and cryptodires/pleurodires to assess the magnitude and significance of shape change from the ancestral condition. Procrustes distances are commonly used to quantify distances between specimens or groups of specimens in Kendall's shape space (e.g. Zelditch et al. 2004). We used the same ancestral landmark configurations that were calculated for the 3D visualization (above), and selected Testudinata node and Testudines node reconstructions. Procrustes distances were calculated between Testudinata/Testudines and the value of the mean point in shape space occupied each by pleurodires and by cryptodires. Goodall's F-test was used to assess the significance of the Procrustes distance between the two points (ancestral node – group mean), and a bootstrap was performed (900 replications) on the F-value to generate a distribution of F-values (at 5% and 1%) that could be compared to the observed value. We also used the same approach to compare the distance in shape space between cryptodires and pleurodires for CV2, CV5 and CV8.

***Disparity Across Phylogeny (DAP)***

To quantitatively explore evolutionary tempo and mode, we used the approach of Harmon et al. (2003) to evaluate how vertebrae shape disparity changed through phylogeny in comparison to trait evolution under a Brownian Motion (BM) model (Fig. 9). Analyses were implemented in the program R (R-Core-Team 2013) using the package 'geiger' (Harmon,

Schulte et al. 2003) and the same phylogenetic framework as used for the phylomorphospace visualizations. This method calculates disparity using average pairwise Euclidean distances between species as a measure of variance in multivariate space [e.g. (Zelditch, Swiderski et al. 2004)]. For each separate data set (CV2, CV5, CV8), PC scores for PC1-PC8, encapsulating 95% of the shape variance, were used for disparity calculations. Following Harmon et al. (2008), relative disparities were calculated by dividing a subclade's disparity by the disparity of the entire clade. Relative subclade disparities were calculated for each node in the phylogeny, progressing up the tree from the root. At each node, the relative disparity value was calculated as the average of the relative disparities of all subclades whose ancestral lineages were present at that time (Harmon, Schulte et al. 2003). Subclades that contain only a small proportion of the total variation will occupy minimally overlapping portions of morphospace and have relative disparity values that are near to 0.0. When relative disparity values are, conversely, close to 1.0, then morphological overlap between the different subclades is extensive. One thousand simulations of morphological diversification were calculated on the phylogenetic framework to assess how mean disparity compared to evolution under a neutral (BM) model. Observed disparity values for the vertebral shape data were plotted alongside the theoretical subclade disparity values generated in the simulations. Clades that have happened to generate higher disparity in the modern fauna are identified in the time slices where the observed subclade disparity line plots above the BM line. In this instance, subclades defined by those time slices will overlap morphospace area occupied by the overall clade.

## Results

### *Distribution of Vertebral Shape*

We defined 25 homologous landmarks (Fig. 2, S2, Table S3) for the cervical vertebrae of 23 species of fossil and living turtles (Table S1) and conducted a principal component analysis (PCA) to compare shape distribution (Fig. 3; excluding the extraordinary CV1s in cryptodires). The plot of PC1 vs. PC2 shows shape separation between the widely scattered stem turtles and pleurodires on the one side and the strongly overlapping cryptodires on the other side (Fig. 3A, cf. Fig. S4). A minimal span tree constructed in PC1-PC2 morphospace shows shape similarities with the following general trend: stem turtles < pleurodires < cryptodires. Cryptodires show the most derived vertebral shapes relative to stem turtles and the cryptodire morphotype is separated from the basal turtle vertebral shape by the intermediate pleurodire morphotype. Generally for most species, adjacent vertebrae in one neck are similar in shape along their sequence (i.e. CV2 is more similar to CV3, which is more similar to CV4, and so on). But some vertebrae of some species are more similar to vertebrae of other species than to their adjacent vertebra in the same vertebral column. Future studies should investigate similarity of particular vertebrae (e.g., CV4) among all species, different vertebrae between different species, and the similarity of vertebrae along the cervical column of particular species. The scope of the present study was to present an overview of shape similarity and of general patterns for all vertebrae (Fig. 3).

Except for dorsal neck flexion, weak correlation exists between vertebral shape and raw mobility between adjacent vertebrae (Fig. S3, Table S8A).

### *Shape Gradients*

In the PC-diagram, the shapes within the sequence of cervical vertebrae show a chaotic pattern along the necks of stem turtles (Fig. 3B, cf. Fig. S1A-D). In cryptodires, a semicircular shape gradient (= morphospace trajectory from CV2 to CV8) is detectable for each species, which indicates a clear anterior-posterior shape gradient along the cervical column in cryptodires (Fig. S1F, cf. Fig. 3C). Pleurodire vertebrae show a partly chaotic pattern, although a weak gradient is present. In contrast to cryptodires, the direction of the gradient is not fixed within pleurodires (Fig. S1E, cf. Fig. 3D).

### *Anterior-Posterior Patterning of Vertebrae*

The shapes of the anterior and posterior halves of each cervical vertebra diverge from each other over the evolutionary history of turtles (Figs 2, S2: landmarks 1-10, 24 and 11-20, 25 respectively; Table S6-7). In stem turtles, the anterior and posterior shapes are similar, whereas a clear anterior-posterior shape divergence is apparent in the vertebrae of all extant turtles (Fig. S5). The shapes of the vertebral halves do not show a strong correlation with measures of raw mobility (Table S8B).

### *Anatomical Shape Change*

*Cervical vertebra 2.* Cervical vertebra 2 did not substantially change in its shape from Testudinata to Testudines. *Proganochelys quenstedti* more or less resembles the ancestral shape (Fig. 5A-J). However, shape drastically changes within Testudines. Cryptodira shows a strong reduction of relative vertebral height (Fig. 5K) and the posterior zygapophyses are flattened (Fig. 5M). The anterior zygapophyses are broader and more robust when compared to the ancestral condition (Fig. 5L, N). The vertebral centra also become more elongated (Fig. 5K, O). Pleurodira also shows reduction in the height of vertebral 2 and an elongation of its

central length (Fig. 5P, T), but not as substantially as found in Cryptodira. The zygapophyses do not show much change compared to the ancestral condition (Fig. 5Q-R). The only mentionable difference of Pleurodira compared to the ancestral Testudines condition is the rostral shift of the transverse processes compared to overall vertebral shape (Fig. 5S-T).

*Cervical vertebra 5.* Cervical vertebra 5 of *P. quenstedti* is relatively higher and anteroposteriorly more compressed than the reconstructed vertebra of Testudinata (Fig. 6A-C). There is not much shape change from Testudinata to Testudines, although the posterior zygapophyses are a bit lower (Fig. 6F-H). Anterior and posterior zygapophyses are lower in Cryptodira when compared to Testudines (Fig. 6K-M). In Cryptodira, the vertebral centra become more elongated and slender (Fig. 7N-O). Shape change of the centrum is similar in Pleurodira (Fig. 6S-T). When compared to Cryptodira, the posterior zygapophyses of this taxon are lower and the distance between these processes of each side become narrower (Fig. 6P, Q).

*Cervical vertebra 8.* As expected, the shape of cervical vertebra 8 shows the most extensive changes through turtle evolution. In *P. quenstedti*, the neural arch is substantially higher and narrower when compared to the reconstructed ancestral condition of Testudinata (Fig. 7A-E). Towards the turtle crown (Testudines), a comprehensive reduction of the vertebra's relative height is apparent (Fig. 7F-J). The relative length of the vertebral centra is larger (Fig. 7F, I-J) and the articular facets of the posterior zygapophyses are expanded in caudal direction (Fig. 7F, I). The only notably change in cervical 8 anatomy between Testudines and Pleurodira is the relative position of the hypophyseal process (Fig. 7P, T), but fundamental anatomical changes occurred towards the ancestral cryptodiran condition (Fig. 8K-O). Although the relative height of CV8 remained the same between Testudines and Cryptodira (Fig. 7K), the relative breadth of the whole vertebra increased extensively. A small increase of central

vertebral length is recognizable as well (Fig. 7K, O). An important change represents the lowering of the posterior zygapophyses relative to the ancestral condition of Testudines.

It is notable for the ancestral conditions of all reconstructed vertebrae that only little shape change occurs in the anatomy of the central articulations (compare to Fig. 2). In general, however, the articulations appear to develop from a more concave, simple procoelous towards a more flat appearance (Figs. 5-7). The different types of central articulations as documented in all extant and some fossil taxa thus appear to represent highly derived and independent recent adaptations.

***Phylomorphospace***

We plotted the phylogenetic topology (Fig. 4) into PC morphospace for CV2, CV5, and CV8 separately. A general direction of shape change can be recognized and a clear distinction of cryptodires (dark blue in Fig. 8) and pleurodires (light blue) is visible for all vertebrae.

For CV2, PC1 reflects the anterior movement of the dorsal crest of the anterior zygapophyses (landmark #24), as well as the distal and medial projection in the posterior central articular process (landmarks #16, 17, 19, 20). These features mainly separate *M. platyceps*, at the negative end of PC1, from cryptodires and pleurodires towards the opposite, positive end of PC1. PC2 mainly separates cryptodires from pleurodires, and is associated with a posterior projection of the distal tips of the transverse processes (landmarks #22 and #23) in cryptodires. PC3 also captures the posterior projection of landmarks #22 and #23 with a small additional outward projection, and hence slight widening of the vertebra. For CV5, shape change along PC1 mainly reflects an outward and posterior projection of the distal tips of the transverse processes, as well as slight anterior projection of the posterior central articular process (landmarks #16-20) in stem taxa compared to cryptodires, located at the negative end of PC1. In contrast, shape change along PC2 captures posterior movement of anterior central

articular process (landmarks #6-10) in cryptodires compared to pleurodires. Shape change for PC3 mainly further accentuates shape changes captured by PC1 and PC2, as well as slight ventral movement of the hypophyseal process. Cryptodires are located at the most negative region of PC1 for CV8, and movement along this axis reflects an outward projection of the anterior and posterior zygapophyses (landmarks #2-3 and #11-13, respectively) in all other taxa, whereas PC2 largely reflects movement of landmarks on the anterior and posterior central articular processes which together act to result in a shortening of the anterior-posterior axis between the centra, mainly capturing differences in shape between *X. qiguensis* and *M. platyceps*. PC3 contributes additional anterior projection of the landmarks located on the transverse processes.

The PC-scores of *M. platyceps* do not fit into the general shape directions in all three data sets (CV2, 5, 8) tested, which indicates a completely different course of shape evolution in this species. This suggests a completely separate morphological diversification of Meiolaniidae. The cow-horned turtles have formed central articulations and survived as recently as 3,000 years ago (White, Worthy et al. 2010). The phylogeny of cow-horned turtles is subject of current research and it remains unclear if they are sister of Paracryptodira, including *C. undatum* and *N. speciosa* (e.g., Anquetin, 2012), or form their own lineage along the turtle stem (Sterli and de la Fuente 2011, Sterli and de la Fuente 2013). Given the long, separate evolution of this taxon, an independent acquisition of formed centra is plausible (see also discussion below). Nevertheless, *M. platyceps* plots relatively close to the basal node of Testudinata, which could also highlight its ancestral vertebral shape and particularly basal position.

Except for CV2, *Naomichelys speciosa* aligns around the node of Testudines, which highlights the uncertain phylogenetic affinity of that species. For CV2, *N. speciosa* aligns with Cryptodira. In the case that *N. speciosa* belongs to the clade Paracryptodira (Hirayama,

Brinkman et al. 2000), our finding could be an indication that Paracryptodira, whose phylogenetic position is also unclear, could actually be a sister group to Cryptodira. In the case *N. speciosa* belongs to Meiolaniidae (as used herein), a similarly separated evolutionary course of that species is conceivable.

*Xinjiangchelys qiguensis* is usual interpreted as a stem-cryptodire (Joyce 2007, Anquetin 2012). The shape of its cervicals (Fig. S2), however, aligns with pleurodires (CV2, CV8) and with cryptodires (CV5) respectively. That condition highlights that at the dawn of modern turtle evolution both modern neck retractions may not have been established but instead successively and independently evolved along the stems of Pleurodira and Cryptodira. The alignment of *X. qiguensis* with cryptodires for CV5 highlights the plesiomorphic condition of that vertebra in both taxa, whereas pleurodires show a major morphological change in CV5 in order to enable the kink of the neck during retraction. The alignment of *X. qiguensis* with pleurodires for CV2 and CV8, accordingly, illustrate the plesiomorphic condition of those vertebrae in both taxa.

Finally, *Chisternon undatum*, whose phylogenetic position is also unclear (Fig. S9), aligns around the stem but shows affinities towards pleurodires. The similar shape of CV5, the 'kink'-vertebra, may indicate that *C. undatum* may have been able to retract its neck in a way like pleurodires do and may designate it to represent a stem pleurodire rather than the sister taxon to Testudines as used herein (Fig. 4).

For CV2, CV5 and CV8, results of Procrustes distances calculations (Table 1) indicate that cryptodires have diverged more in shape (i.e. greater Procrustes distance) from the reconstructed ancestral shape of Testudinata and Testudines than have pleurodires. Notably, the greatest Procrustes distances were for CV5, in which both pleurodires and cryptodires differed significantly from Testudines and Testudinata. Cryptodires were also found to be significantly different from ancestral shapes for CV2 and CV8 whereas pleurodires showed

less shape change and non-significant F-values (Table 1). Tests for distances between group means of cryptodires and pleurodires were significant for all cervicals reflecting the clear division seen in the phylomorphospace plots, and most strongly for CV5.

### *Disparity Across Phylogeny*

We evaluated how vertebrae shape disparity changed through phylogenetic time in comparison to trait evolution under a Brownian Motion (BM) model (Fig. 9). Initially, disparity is high, reflecting the disparity between morphologically divergent stem forms. Following the emergence of crown turtles, at the origin of major extant turtle clades, disparity declines, falling below that expected under neutral (Brownian) evolution, with a slight increase toward the present. Subclades do not generally tend to generate higher disparity in the modern fauna than would be expected under the Brownian motion model, as indicated by a considerable number of time slices having disparity values (Fig. 9, solid line) below those generated from BM simulations (Fig. 9, dashed line). Notably, CV2 and CV8 show an initial high level of disparity above the BM simulation line, whereas CV5 disparity does not show this initial peak, remaining close to or below the BM simulation line.

## Discussion

### *Vertebral Evolution within Testudinata*

Even though the two primary types of neck retraction of modern turtles featured prominently in early phylogenetic debates, Williams (1950) was the first to systematically survey the cervical osteology of turtles and to formulate characters, of which most pertained to the highly variable morphology of the cervical centra. In the more recent cladistic literature, characters derived from this study are consistently featured, and most authors profit directly

from Williams' work. Initially, workers focused on scoring characteristic cervical central formulae (e.g., (Gaffney and Meylan 1988, Meylan and Gaffney 1989, Gaffney 1996, Shaffer, Meylan et al. 1997, Brinkman and Wu 1999, Hirayama, Brinkman et al. 2000)), but Joyce (2007) and Sterli and de la Fuente (2011) suggested methods on how to score all possible morphological characteristics of the centra seen in extant turtles in a series of discrete characters. Herein, we decided to utilize a geometric morphometric approach to characterize the shape of the neck vertebrae of fossil turtles, pleurodires, and cryptodires.

Results of our disparity across phylogeny analyses provide support for hypothesis 1, which states that the disparity of vertebral shape change was high when modern turtles arose (Fig. 9). However, the disparity of vertebral shape was already comparably high in the ground pattern of Testudinata, which highlights the large morphological diversity of stem turtle taxa in the Mesozoic. After the rise of modern turtles (Testudines), disparity declined rapidly suggesting a stabilization of vertebral anatomy within the major turtle groups. Later in evolution, the disparity of modern turtles increased slightly from around the most recent 35% of relative time, indicating that shape disparity for subclades was slightly higher in the modern fauna than expected under a neutral (BM) model. This result may in part mirror more recent independent morphological adaptations, though it should be noted that peaks at the most recent 10% of the plot may be attributed to 'tip overdispersion' due to missing terminal taxa. Of note, the plots for CV2 and CV8 show broadly similar patterns of disparity that are different from CV5, the latter showing levels of disparity that more closely align with neutral evolution. This result may tentatively reflect a greater evolutionary lability of CV2 and CV8 in contrast to CV5. While the link between disparity, constraint/facilitation and capacity for morphological change is topical in studies of morphological evolution, we may suggest that lower levels of disparity in CV5 could relate to selective pressure to retain a functional and stable mid-neck region whereas more extensive shape change in CV2 and CV8 reflects key

modifications required by the distinct neck retraction modes.

Vertebral shape distribution shows a clear phylogenetic pattern as all cervical vertebrae of crown Cryptodira and Pleurodira are separated in morphospace (Figs 3A, 8). Although the fossil turtles *Proganochelys quenstedti, Meiolania platyceps,* and *Naomichelys speciosa* together occupy a large portion of morphospace, they nevertheless are closely associated with each other, which suggests they represent the early diversification of turtles. *Chisternon undatum*, which is phylogenetically situated near the base of crown Testudines (Joyce 2007, Anquetin 2011, Sterli and de la Fuente 2013), may represent a stem pleurodire, whereas *Xinjiangchelys qiguensis*, which is typically placed with other xinjiangchelyid turtles along the stem of Cryptodira (Joyce 2007, Anquetin 2012), is intermediate between pleurodires and cryptodires (Fig. 3) but generally shows a plesiomorphic shape in all vertebrae (Fig. 8).

To reach the cryptodiran morphospace in the minimal span tree from the basal turtle morphospace, it is necessary to 'cross' the pleurodiran morphospace (Fig. 3A: red lines). This suggests that cryptodires show the most derived vertebral shapes, whereas pleurodires possess a vertebral shape that is closer to the plesiomorphic condition, and as such is intermediate between stem turtles and cryptodires. It therefore appears that pleurodires were able to establish their unique retraction mode by acquiring a few precursory modifications to the neck (see below). These early pleurodiran-like modifications in the stem were also the prerequisite to establishing the cryptodiran vertebral shape afterwards. These modifications are also mirrored in the ancestral shape reconstruction that we performed (Fig. 5-7), as well as results from calculations of Procrustes distances in shape space. For CV2, CV5 and CV8, cryptodires diverged more (=greater Procrustes distance) from the ancestral shape in shape space than did pleurodires, and this divergence was significantly greater than expected by random chance (<0.05) (Table 1). Generally, pleurodires show a more ancestral anatomy of their vertebrae when compared to cryptodires and only the middle vertebrae (as exemplified for CV5, Fig. 6)

show a notable change in the orientation of the posterior zygapophyses when compared to the ancestral shape of Testudines. Similarly, for pleurodires only the Procrustes distance values for CV5 showed a significantly greater divergence in shape from the ancestral Testudinata shape (Table 1).

The cervical joints of stem turtles are not yet specialized and therefore, when PC-scores are successively connected ("shape curve"), the shapes of their vertebrae are randomly distributed along the neck within morphospace (Fig. 3B). The neck of cryptodires, by contrast, is characterized by cervical joints that become increasingly more mobile towards the posterior (Table S2). This observation may explain the orderly anterior-posterior shape patterning that their vertebrae form in morphospace (Fig. 3C). Conversely, the necks of pleurodires show the greatest amount of mobility between cervicals 4 and 5 (Herrel, Van Damme et al. 2008), and this specialization is reflected by the notable kinks in their "shape curves" (Fig. 3D).

***Cryptodira vs. Pleurodira***

We can confirm hypothesis 2, which states that the ancestral vertebral shapes of Testudinata and Testudines, in many aspects, are strikingly different from Pleurodira and Cryptodira, indicated by the significant departure of group mean pleurodire and cryptodire shape from ancestral shapes in shape space (Table 1). Cryptodira have diverged more than Pleurodira, though both have diverged from one ancestor and from one another (Table 1). The signal is much weaker for Pleurodira vs. Testudines particularly for CV2 and CV8 (this is not significant, whereas CV5 is).

Besides minor obvious differences (Fig. 5-7), the cryptodiran vertebrae are generally more compressed dorsoventrally when compared to pleurodires (e.g., Fig. 5M vs. 5R). Moreover, the articular facets of the zygapophyses are either broad (Cryptodira) or narrow (Pleurodira). Finally, the orientation of the posterior zygapophyses of CV8 is rather straight in pleurodires,

whereas it is ventrally bent in cryptodires, a separation that is also visible and captured in shape change along PC1 (Fig. 9C). All of these modifications in the cervical column clearly illustrate the adaptation of vertebrae to either type of neck retraction. Whereas general retraction is enabled by the *musculus retrahens capiti collique*, which attaches ventrally to the head and ventrolaterally to the neck of all turtles (Herrel, Van Damme et al. 2008, Werneburg 2011), several other muscles can broadly attach to the upper part of the vertebrae in cryptodires to enable dorsal bending of the cervical column during cryptodiran retraction (Herrel, Van Damme et al. 2008). Therefore, a broad vertebra is advantageous. Similarly, the tall vertebrae of pleurodires are best adapted to laterally attaching muscles (Herrel, Van Damme et al. 2008, Werneburg 2011). The higher the vertebrae, the less dorsoventral mobility is possible without risking a large amount of disarticulation, although some disarticulation was observed among extant taxa (Werneburg, Hinz et al. in press). And the narrower the zygapophyses, the higher the lateral degree of freedom is between adjacent vertebrae (Werneburg, Hinz et al. in press). Finally, the modification of the posterior zygapophyses in cryptodires enables a unique articulation with the first carapacial vertebra (Dalrymple 1979) that permits vertical retraction of the cervical column into the turtle shell (Fig. 1A).

The advent of the modern pleurodiran and cryptodiran neck retraction mechanisms is generally thought to correlate tightly with the acquisition of "formed cervical centra" (Fig. 2D-H), but it is apparent from all phylogenies that formed centra emerged at least two more times within Testudinata in addition to Pleurodira and Cryptodira, in particular along the stem lineage leading to the cow-horned turtle *Meiolania platyceps* (Gaffney and Meylan 1988, Gaffney 1996, Hirayama, Brinkman et al. 2000, Joyce 2007, Sterli and de la Fuente 2011) and within the North American clade Baenidae (Joyce 2007, Danilov and Parham 2008, Tong, Claude et al. 2009). However, the literature has been decisively silent concerning speculations

on whether these taxa could withdraw their head or whether their neck had a specific plane of movement.

Our observations show that there is no simple correlation between the shape of vertebral articulations and the amount of mobility of adjacent vertebrae. Also, the measured lengths of the vertebrae and the zygapophyseal angles have no overwhelming influence on the amount of mobility (Table S2). The reconstruction of ancestral vertebral shapes only resulted in minute changes of the simple shape of central articulations towards modern turtle evolution and highlights the independent acquisition of formed vertebrae within separate extant and fossil lineages. We therefore conclude that a variety of anatomical characteristics as a whole define the extent of intervertebral mobility, not the presence of formed centra alone [please note that Werneburg et al. (in press) have shown that intervertebral disk does not have any important influence on the range of mobility].

***Ancestral neck retraction***

We can support hypothesis 3, which states that stem turtles were not able to retract their necks in the way that extant cryptodires and pleurodires do. As mentioned above, there are fundamental differences in vertebral anatomy that can be assigned to either one style of modern neck retraction. This is particularly obvious for cryptodires with their flattened vertebrae and the modified posterior zygapophyses of their CV8.

The vertebral shape of advanced stem turtles, such as *Chisternon undatum*, greatly resembles that of pleurodires and it is therefore tempting to infer a pleurodiran-like neck retraction for this taxon. However, we note three important details that are incongruous with full pleurodire type of retraction. First, whereas advanced stem turtles have homogenous posterior zygapophyses, the posterior zygapophyses in the middle portion of the cervical column are different from the rest in pleurodires. These autapomorphic modifications are likely related to

the strong kink apparent in pleurodires during retraction (Fig. 1B). Second, the orientation of the transverse process, particularly in the anterior vertebrae, is different in pleurodires compared to the Testudines-node (Fig. 5, captured along PC2, Fig. 9B). This is likely because several important neck and head associated muscles autapomorphically insert in the anterior region of the neck in pleurodires. These are important for internal neck flexion and for the lateral flexion of the head during pleurodire retraction (Werneburg 2011). Third, as in cryptodires, pleurodires show elongation of the vertebral centra compared to the ancestral Testudines-shape, which in return results in a narrower shape of the vertebral column and greater flexibility (Werneburg, Hinz et al. in press). A longer neck, in return, is particularly exposed to predators and, consequently, selection pressure towards the highly specific styles of modern retractions only needs to be expected for Testudines.

The reconstruction of ancestral vertebral shapes shows that many aspects of the vertebral anatomy only gradually changed across stem turtle evolution. And, as mentioned above, the shape of the whole vertebra has to be taken into account when explaining mobility between adjacent vertebrae. As already shown by Werneburg et al. (in press), slight internal rotation among the neck vertebrae should have enabled a primitive kind of neck retraction in the fossil turtle *P. quenstedti* (Fig. 1C). This type of retraction would have differed drastically from the plain, non-rotated vertical course of retraction found in cryptodires (Fig. 1A). However, a certain similarity cannot be rejected between pleurodiran retraction and the proposed stem turtle retraction (Fig. 1B-C) given that pleurodiran retraction also requires internal rotation of adjacent neck vertebrae. As mentioned above, the necks of pleurodires show a certain similarity to the vertebral shape inherited from stem turtles. The necks of pleurodires, which are elongated compared to stem turtles, however, are withdrawn in an S-shape under the shell. For that a strong "kink" had to evolve in the mid region, which requires the detected vertebral modifications (Fig. 6). However, given that the lateral head-tuck of stem turtles already

demanded great lateral mobility to both body sides at the base of the neck (CV8/DV1 articulation), pleurodiran retraction did not demand many changes to this region of the vertebral column. The key innovation of pleurodires, hence, lies in higher mobility of the mid cervical region only. Given our reconstructions, one may imagine a subsequent higher mobility of the neck along stem turtle evolution towards more pleurodiran-like neck flexibility during retraction. The long transverse processes that are found in advanced stem turtles, such as *Chisternon undatum* (Fig. S1C), may have served as lateral muscle attachment sites and may support that hypothesis of higher lateral flexibility.

The ancestral lateral tuck of stem turtles and pleurodiran-like advances during stem turtle evolution may actually have also been the precondition for the vertical retraction found in cryptodires. Increasing mobility between the cervical vertebrae appears to have been obtained in the turtle stem lineage. This mobility is associated with comprehensive anatomical changes in the vertebrae. And these changes, in return, appear to be the precondition for the dorsal flexibility between CV1 to CV7 and the ventral flexibility between CV8 and DV1 that are required for cryptodiran retraction. We hypothesize that, associated with increasing general neck mobility and change of vertebral shape, a successive rotation of the laterally retracted stem turtle neck towards the saggitally retracted neck of cryptodires happened through turtle evolution. In that regard, pleurodires show a less advanced adaptation to retraction compared to cryptodires. This hypothesis is supported by the fact that extant cryptodires do not necessarily show a straight saggital neck position during retraction but can rather show some degree of sideward motion (Werneburg, Hinz et al. in press). That highlights the anatomical, functional, and evolutionary potential of neck vertebral shape.

Whereas cryptodires completely retract the neck and head inside the body wall, pleurodires ancestrally expose still much of the lateral part of the head and neck to predators. Although we do not know the specific selection pressure on turtles that lead to the acquisition of the

turtle shell, we can conclude that modern neck retraction enabled a further protection against predators relative to the simple head tuck found in stem turtles.

**Conclusions**

1. Using a comprehensive geometric morphometric approach, we identified the main axes of vertebral shape change in a broad sample of extant and fossil turtle species. We traced the evolution of vertebral shape along the stem line of turtles and were able to reconstruct the ancestral anatomy of different clades. These reconstructions permit a detailed association of shape and function during neck retraction of pleurodires, cryptodires, and stem turtles.
2. Disparity of vertebral shape was high in early turtle evolution and declined after the two modern clades emerged, reflecting a stabilization of the acquired morphotypes. Towards recent time, disparity slightly increased reflecting the recent diversification of modern groups.
3. In order to reach the modern cryptodire vertebral shape, stem turtle had to pass a "pleurodiran-like" morphospace. In that regard, pleurodires generally show a more ancestral vertebral shape than cryptodires do.
4. Ancestral shape reconstruction reveals that the pleurodiran and cryptodiran retraction did not evolve independently from one another. The pleurodiran retraction represents a slight modification of the lateral tuck found stem turtles. Shape change mainly occurred in the middle third of the neck to allow fully kinking the vertebral column and better hide the elongated neck under the shell.
5. The neck vertebral shapes of cryptodires and pleurodires are clearly distinguishable from one each other and show clear correspondence to either one mode of retraction. Those specific combinations of vertebral adaptations were not present in stem turtles, which were not able to retract their necks like modern turtles do.

6. Formed vertebral centra are shown to represent just one factor for higher neck mobility and – as illustrated for stem turtles – are not necessarily needed for retraction.
7. General changes in vertebral anatomy through stem turtle evolution can be associated with higher mobility and more effective retraction of the neck. We therefore hypothesize that the ancestral lateral motion found in the ancestral crown turtle gradually evolved into the vertical motion found in cryptodires.

**Acknowledgements**

We would like to thank Irina Ruf (Universität Bonn), Virginie Volpato (Senckenberg Museum Frankfurt), Herbert Schwarz (Universitätsklinikum Tübingen), Jan Prochel, Juliane Hinz, and Katerina Harvati-Papatheodorou (Universität Tübingen) for help with acquisition and processing of CT-data. Carl Mehling (AMNH), Rainer Schoch (SMNS), Gunther Köhler, Linda Acker (SMF), and Philipe Havlik (Paleontological Collection, Tübingen) generously provided access to fossils and extant specimens in their care. For discussion we thank Robin Beck. Frank Anderson, Norm MacLeod, Ken Angielczyk, Juliana Sterli, and one anonymous reviewer provided constructive suggestions that helped improve the manuscript. This project was funded by a grant from the Deutsche Forschungsgemeinschaft to WGJ (JO 928/1). LABW is supported by the Swiss National Science Foundation (SNF) (PBZHP3_141470 and P300P3_151189). IW also wishes to acknowledge Marcelo R. Sánchez-Villagra (Universität Zürich), who supported this study with SNF-grant 31003A_149605, and the Swiss Palaeontological Society for funding.

## References


Anquetin, J. (2011). "Evolution and palaeoecology of early turtles: a review based on recent discoveries in the Middle Jurassic." Bulletin De La Societe Geologique De France 182(3): 231-240.

Anquetin, J. (2012). "Reassessment of the phylogenetic interrelationships of basal turtles (Testudinata)." Journal of Systematic Palaeontology 10(1): 3-45.

Baur, G. (1890). "On the Classification of the Testudinata." The American Naturalist 24(282): 530-536.

Brinkman, D. B. and X. C. Wu (1999). "The skull of Ordosemys, an Early Cretaceous turtle from Inner Mongolia, People's Republic of China, and the interrelationships of Eucryptodira (Chelonia, Cryptodira)." Paludicola 2: 134-147.

Dalrymple, G. H. (1979). "Packaging problems of head retraction in trionychid turtles." Copeia(4): 655-660.

Danilov, I. G. and J. F. Parham (2008). "A reassessment of some poorly known turtles from the middle Jurassic of China, with comments on the antiquity of extant turtles." Journal of Vertebrate Paleontology 28(2): 306-318.

Dyreson, E. and W. P. Maddison (2003). "Rhetenor package for morphometrics for the Mesquite system."

Gaffney, E. S. (1975). "A phylogeny and classification of the higher categories of turtles." Bulletin of the American Museum of Natural History 155(5): 387-436.

Gaffney, E. S. (1975). "A revision of the side-necked turtle Taphrosphys sulcatus (Leidy) from the Cretaceous of New Jersey." American Museum Novitates 2571: 1-24.

Gaffney, E. S. (1990). "The comparative osteology of the Triassic turtle Proganochelys." Bulletin of the American Museum of Natural History 194: 1-263.

Gaffney, E. S. (1996). "The postcranial morphology of Meiolania platyceps and a review of the Meiolaniidae." Bulletin of the American Museum of Natural History 229: 1-166.

Gaffney, E. S. and P. A. Meylan (1988). A Phylogeny of Turtles. The Phylogeny and Classification of the Tetrapods. Volume 1: Amphibians, Reptiles, Birds. M. J. Benton. Oxford, Clarendon Press. Special Vol. 35A: 157-219.

Gaffney, E. S., T. H. Rich, P. Vickers-Rich, A. Constantine, R. Vacca and L. Kool (2007). "Chubutemys, a new eucryptodiran turtle from the Early Cretaceous of Argentina, and the relationships of the Meiolaniidae." American Museum Novitates 3599: 1-35.

Gower, J. C. (1975). "Generalized procrustes analysis." Psychometrika 40: 33-51.

Gunz, P., P. Mitteroecker, S. Neubauer, G. W. Weber and F. L. Bookstein (2009). "Principles for the virtual reconstruction of hominin crania." Journal of Human Evolution 57 57: 48.

Hammer, O., D. A. T. Harper and P. D. Ryan (2001). "Past: palaeontological statistics software package for education and data analysis." Palaeontologia Electronica 4(1, art. 4): 9pp.

Harmon, L. J., J. A. Schulte, A. Larson and J. B. Losos (2003). "Tempo and mode of evolutionary radiation in iguanian lizards." Science 301: 961-964.

Harmon, L. J., J. T. Weir, C. D. Brock, R. E. Glor and W. Challenger (2008). "GEIGER: investigating evolutionary radiations." Bioinformations 24(1): 129-131.

Hay, O. P. (1908). "The fossil turtles of North America." Carnegie Institution of Washington 75: 1-568.

Herrel, A., J. Van Damme and P. Aerts (2008). Cervical Anatomy and Function in Turtles. Biology of Turtles. J. Wyneken, M. H. Godfrey and V. Bels. Boca Raton, London, New York, CRC Press: 163-185.

Hirayama, R., D. B. Brinkman and I. G. Danilov (2000). "Distribution and biogeography of nonmarine Cretaceous turtles." Russian Journal of Herpetology 7: 181-198.

Jackson, D. A. (1993). "Stopping rules in principal components analysis: a comparison of heuristical and statistical approaches." Ecology 74 74: 2204-2214.

Joyce, W., J. Sterli and S. Chapman (in press). "The skeletal morphology of the solemydid turtle Naomichelys speciosa from the early Cretaceous of Texas." Journal of Paleontology.

Joyce, W. G. (2007). "Phylogenetic relationships of Mesozoic turtles." Bulletin of the Peabody Museum of Natural History 48(1): 3-102.

Joyce, W. G., J. F. Parham and J. A. Gauthier (2004). "Developing a protocol for the conversion of rank-based taxon names to phylogenetically defined clade names, as exemplified by turtles." Journal of Paleontology 78(5): 989-1013.

Joyce, W. G., J. F. Parham, T. R. Lyson, R. C. M. Warnock and P. C. J. Donoghue (2013). "A divergence dating analysis of turtles using fossil calibrations: an example of best practice." Journal of Paleontology 87(4): 612-634.

Joyce, W. G. and J. Sterli (2012). "Congruence, non-homology, and the phylogeny of basal turtles." Acta Zoologica 93(2): 149-159.

Lydekker, R. (1889). Catalogue of the Fossil Reptilia and Amphibia in the British Museum (Natural History), Pt. 3, Chelonia. . London, Longmans.

Maack, G. (1869). "Die bis jetzt bekannten fossilen Schildkröten und die im oberen Jura bei Kehlheim (Bayern) und Hannover neu aufgefunden ältesten Arten derselben." Palaeontographica 18: 193-336.

Maddison, W. P. (1991). "Squared-change parsimony reconstructions of ancestral states for continuous-valued characters on a phylogenetic tree." Systematic Zoology 40: 304-314.

Maddison, W. P. and D. R. Maddison (2011). "Mesquite: a modular system for evolutionary analysis. Version 2.75, http://mesquiteproject.org."

Meylan, P. A. and E. S. Gaffney (1989). "The skeletal morphology of the Cretaceous cryptodiran turtle, Adocus, and the relationships of the Trionychoidea." American Museum Novitates 2941: 1-60.

Müller, J., T. M. Scheyer, J. J. Head, P. M. Barrett, I. Werneburg, P. G. P. Ericson, D. Pol and M. R. Sánchez-Villagra (2010). "Homeotic effects, somitogenesis and the evolution of vertebral numbers in recent and fossil amniotes." PNAS 107: 2118-2123.

Parr, W., S. Wroe, U. Chamoli, H. S. Richards, M. R. McCurry, P. D. Clausen and C. McHenry (2012). "Toward integration of geometric morphometrics and computational biomechanics: new methods for 3D virtual reconstruction and quantitative analysis of Finite Element Models." Journal of Theoretical Biology 301: 1-14.

R-Core-Team (2013). "R: A language and environment for statistical computing. R Foundation for Statistical Computing, Vienna, Austria. ISBN 3-900051-07-0, URL: http://www.R-project.org/."

Rohlf, J. (1990). Rotational fit (Procrustes) methods. Proceedings of the Michigan Morphometrics Workshop. J. Rohlf and F. L. Bookstein. Ann Arbor, Special Publication Number 2. The University of Michigan Museum of Zoology: 227-236.

Rohlf, J. and D. Slice (1990). "Extensions of the Procrustes method for the optimal superimposition of landmarks. ." Systematic Zoology 39: 40-59.

Romer, A. S. (1956). Osteology of the Reptiles. Chicago, London, The University of Chicago Press.

Scanlon, T. C. (1982). Anatomy of the neck of the western painted turtle (Chrysemys picta belli Gray; Reptilia, Testudinata) from the perspective of possible movements in the region PhD-thesis, The University of Michigan.

Shaffer, H. B., P. Meylan and M. L. McKnight (1997). "Tests of turtle phylogeny: Molecular, morphological, and paleontological approaches." Systematic Biology 46: 234-268.

Sidlauskas, B. (2008). "Continuous and Arrested Morphological Diversification in Sister Clades of Characiform Fishes: A Phylomorphospace Approach." Evolution 62(12): 3135-3156.

Simpson, G. G. (1938). "Crossochelys, Eocene homed turtle from Patagonia." American Museum Novitates 4: 221-254.

Sterli, J. and M. S. de la Fuente (2011). "A new turtle from the La Colonia Formation (Campanian–Maastrichtian), Patagonia, Argentina with remarks on the evolution of the vertebral column in turtles." Palaeontology 54(1): 63-78.

Sterli, J. and M. S. de la Fuente (2011). "Re-description and evolutionary remarks on the Patagonian horned turtle Niolamia argentina Ameghino, 1899 (Testudinata, Meiolaniidae)." Journal of Vertebrate Paleontology 31(6): 1210-1229.

Sterli, J. and M. S. de la Fuente (2013). "New evidence from the Palaeocene of Patagonia (Argentina) on the evolution and palaeo-biogeography of Meiolaniformes (Testudinata, new taxon name)." Journal of Systematic Palaeontology 11(7): 835-852.

Thomson, R. C. and H. B. Shaffer (2010). "Sparse supermatrices for phylogenetic inference: taxonomy, alignment, rogue taxa, and the phylogeny of living turtles." Systematic Biology 59(1): 42-58.

Tong, H., J. Claude, W. Naksri, V. Suteethorn, E. Buffetaut, S. Khansubha, K. Wongko and P. Yuangdetkla (2009). "Basilochelys macrobios n. gen. and n. sp., a large cryptodiran turtle from the Phu Kradung Formation (latest Jurassic-earliest Cretaceous) of the Khorat Plateau, NE Thailand." Geological Society, London, Special Publications 315(1): 153-173.

Werneburg, I. (2011). "The cranial musculature in turtles." Palaeontologia Electronica 14(2): 15a:99 pages.

Werneburg, I., J. K. Hinz, M. Gumpenberger, V. Volpato, N. Natchev and W. G. Joyce (in press). "Modeling neck mobility in fossil turtles." Journal of Experimental Zoology, Part B, Molecular and Developmental Evolution.

White, A. W., T. H. Worthy, S. Hawkins, S. Bedford and M. Spriggs (2010). "Megafaunal meiolaniid horned turtles survived until early human settlement in Vanuatu, Southwest Pacific." Proceedings of the National Academy of Sciences of the United States of America 107(35): 15512-15516.

Wiley, D. F., N. Amenta, D. A. Alcantara, D. Ghosh, Y. J. Kil, E. Delson, W. Harcourt-Smit, F. , J. Rohlf, K. St. John and B. Hamann (2005). "Evolutionary morphing." Proceedings of the IEEE Visualization (VIS'05): 431-438.

Williams, E. E. (1950). "Variation and selection in the cervical central articulations of living turtles." Bulletin of the American Museum of Natural History 94(9): 509-561.

Zelditch, M. L., D. L. Swiderski, H. D. Sheets and W. L. Fink (2004). Geometric morphometrics for biologists: a primer. Amsterdam, Elsevier Academic Press.

## Figure Legends

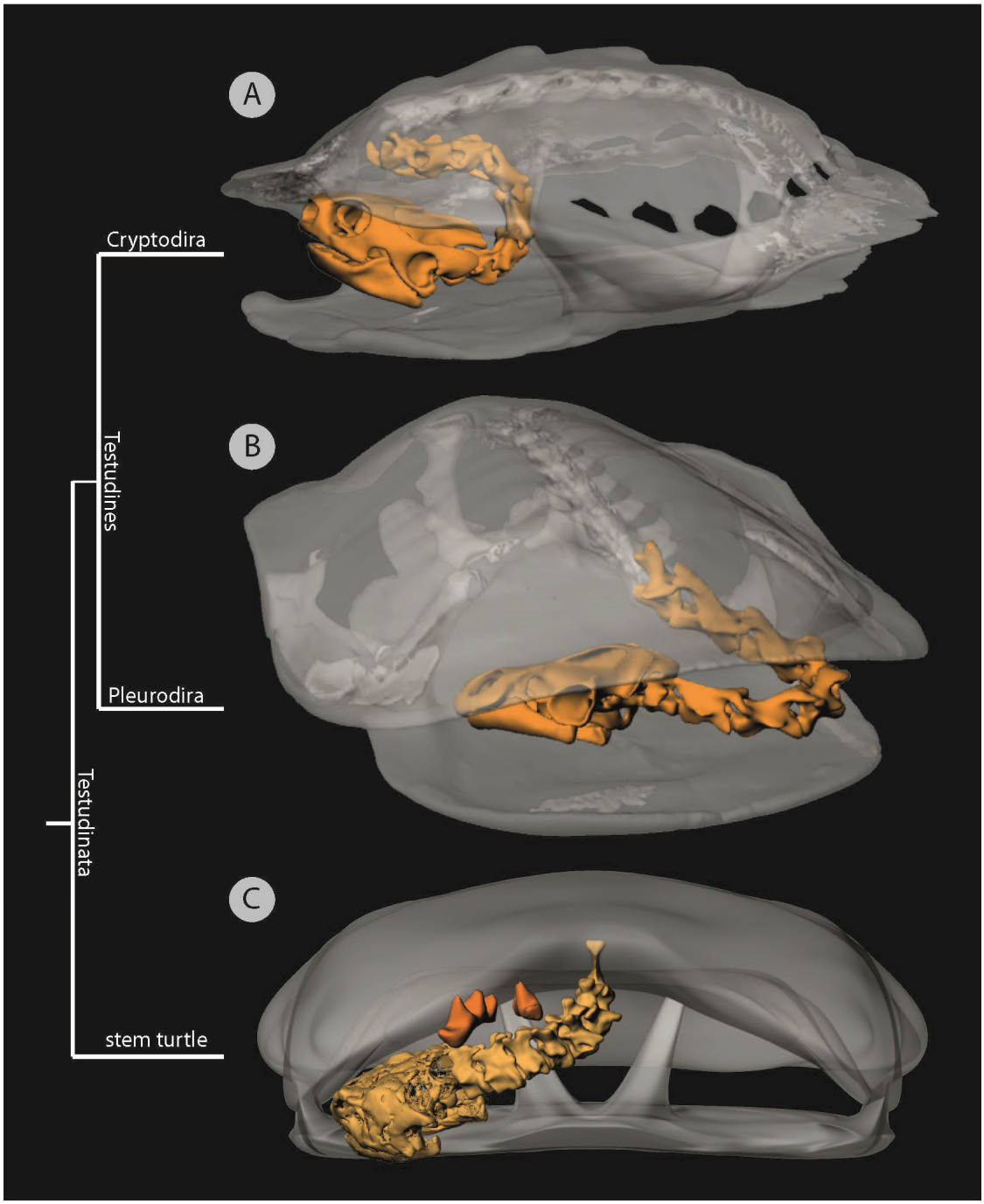


**Fig. 1.** Modes of neck retraction in turtles. **A)** Cryptodiran retraction mode exemplified for *Graptemys pseudogeographica*, the neck is retracted in a vertical plane; **B)** pleurodiran retraction mode exemplified for *Phrynops hilarii*, the neck is retracted in a horizontal plane; **C)** retraction mode of the fossil †*Proganochelys quenstedti* as proposed and modeled by Werneburg, Hinz et al. (in press), the neck is laterally tucked under the shell by small rotation

and ventral movement of adjacent vertebrae - note the osteoderms on the neck that serve for additional defense, the minute neck ribs of that species are not shown but are considered not to impair neck retraction; **A-B)** derived from medical CT-scans of living specimens, shown in frontolateral views; **C)** derived from µCT-scans and 3D-modelling, frontal view. Images modified from Werneburg, Hinz et al. (in press); original artwork by Juliane K. Hinz (University of Tübingen) and I.W.

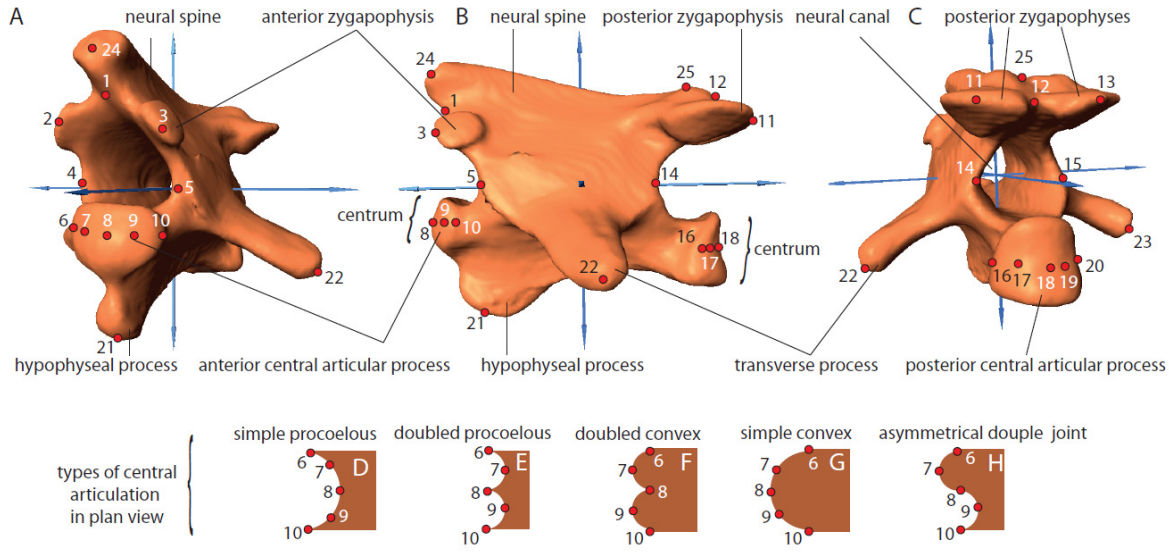


**Fig. 2.** Vertebral terminology and definition of landmarks. **A-H)** Landmarks for 3D-morphometric analysis of vertebral shapes as exemplified by the 7th cervical vertebra (CV7) of the pleurodire *Podocnemis unifilis* (SMF 55470). Screenshots taken with the software Landmark. Nomenclature follows Scanlon (Scanlon 1982). Homologization of landmarks follows (Williams 1950) and (Joyce 2007) **A)** left anterolateral view, **B)** left lateral view, **C)** left posterolateral view, slight dorsal. In pleurodires, the anterior zygapophyses (landmarks 2-3) can unite with landmarks 1 and 24 and, in those cases, they are defined with the same coordinate. **D-H)** Schematic dorsal view of the anterior central articular process with different kinds of articulation and the related landmark definitions. For landmark description see Table S3. For the same landmarks illustrated using *Xinjiangchelys qiguensis* see Fig. S2.

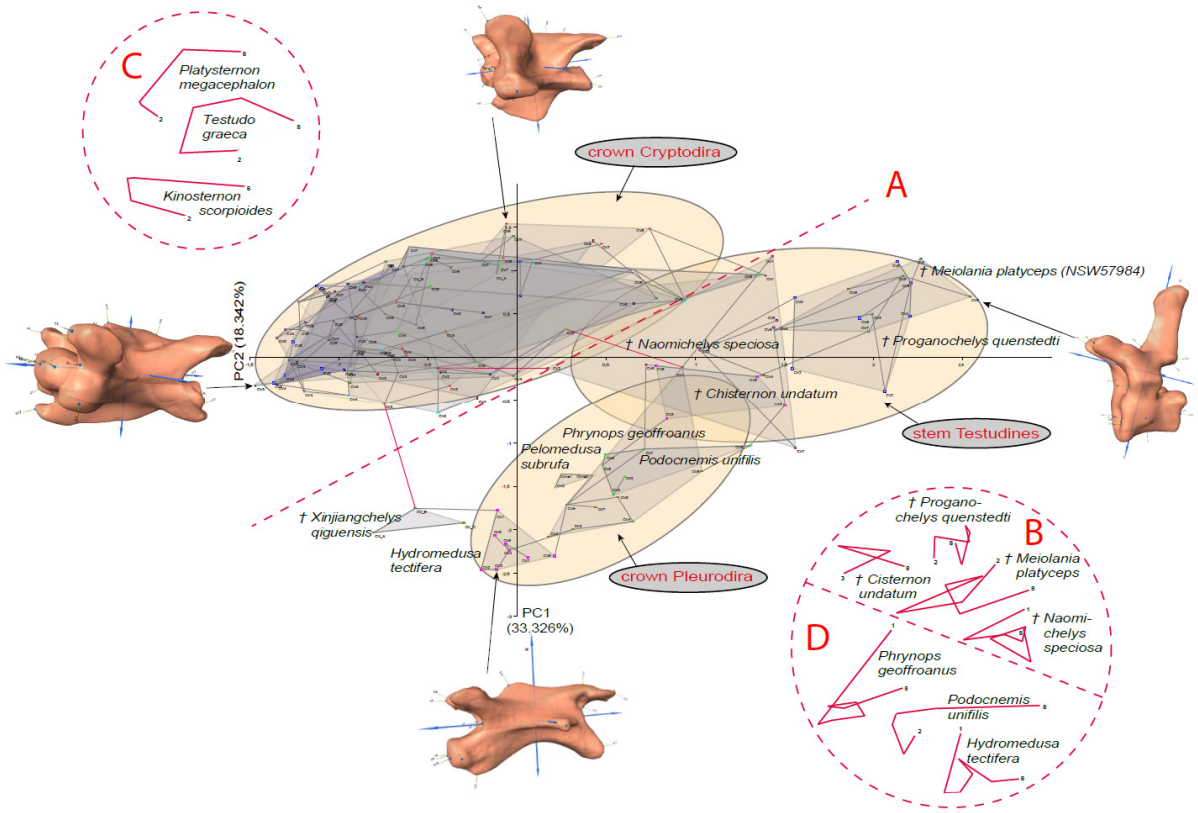


**Fig. 3.** Geometric morphometric analysis of the 3D-shape of 146 cervical vertebrae (CV) with 25 landmarks each. The 3D-shapes of the vertebrae show a distinct pattern. All vertebrae of fossil taxa and pleurodires are separated from crown cryptodires (**A**). Moreover, whereas a variable shape gradient exists from anterior to posterior vertebrae in fossils and pleurodires (**B, D**), the shapes of the neck vertebrae in crown cryptodires show a clear spatial alignment into a semicircle along the anterior to the posterior vertebrae (**C**). The minimum span tree (minimal shape difference) bridges the pleurodire/fossil-morphospace with the crown cryptodire morphospace at two points – between CV-B of *Xinjiangchelys qiguensis (*stem cryptodire) and CV-3 of *Cuora mouhotii* (crown cryptodire) as well as between CV-1 of *Phrynops geoffroanus* and CV-2 of *Testudo hermanni*. *X. qiguensis* has the largest shape similarity to *Hydromedusa tectifera*. These shape similarities and the stem cryptodiran position of *X. qiguensis* speak for a differentiation of the cryptodire type from the pleurodiran morphotype, which itself differentiated from the stem turtle morphotype (stem turtle morphotype → pleurodiran morphotype → cryptodiran morphotype). The clear anterior-

posterior shape gradient of the vertebrae as seen in cryptodires (**C**) is only slightly indicated in pleurodires (**D**) with *Podocnemis unifilis* resampling the cryptodire orientation and *Hydromedusa tectifera* and *Phrynops geoffroanus* showing a reverse gradient orientation. For detailed PC1/PC2, PC1/PC3, and PC2/PC3 diagrams see Fig. S4.

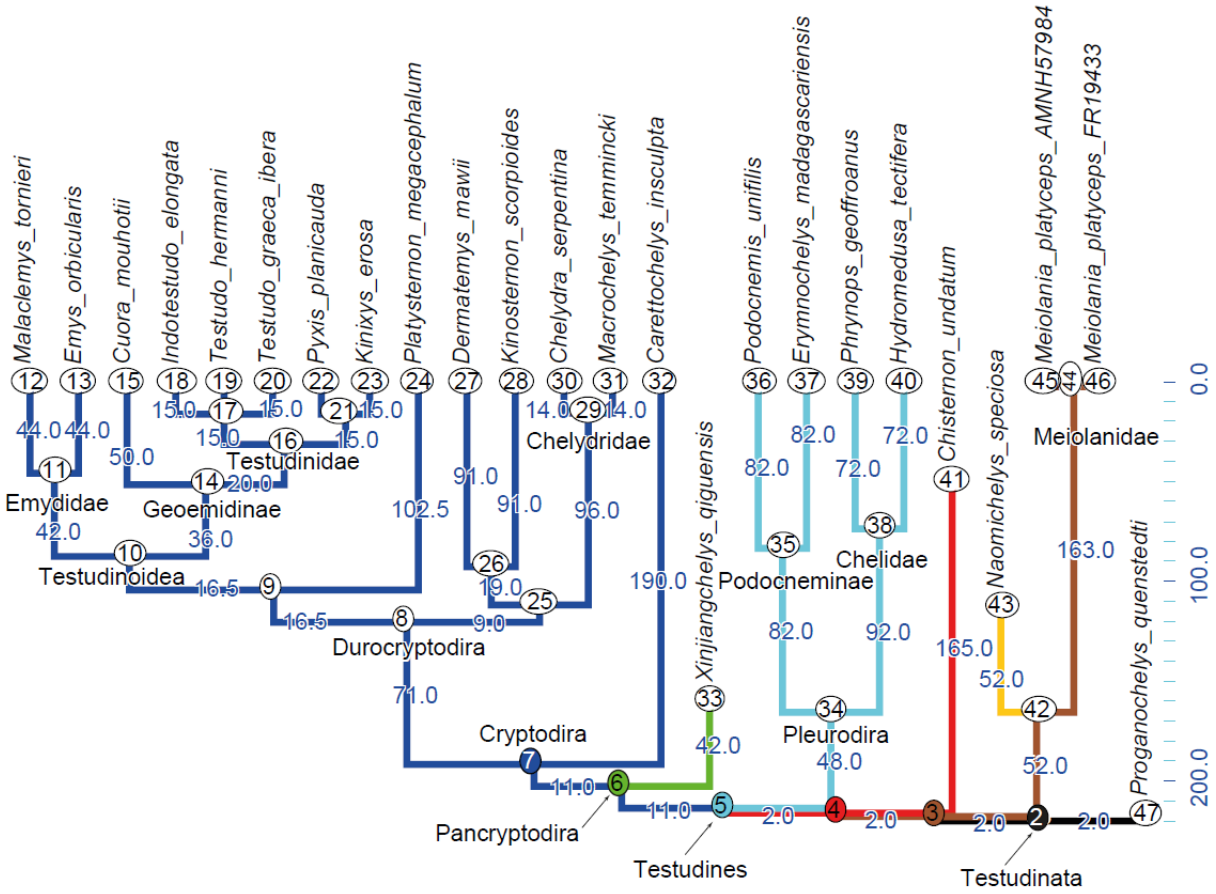


**Fig. 4.** Topology and species and specimens used herein. Time calibrated topology (in million years; see Table S9) with a meiolaniid affinity for *Naomichelys speciosa*. Blue numbers = branch lengths. Units in the time scale equal 10 my.

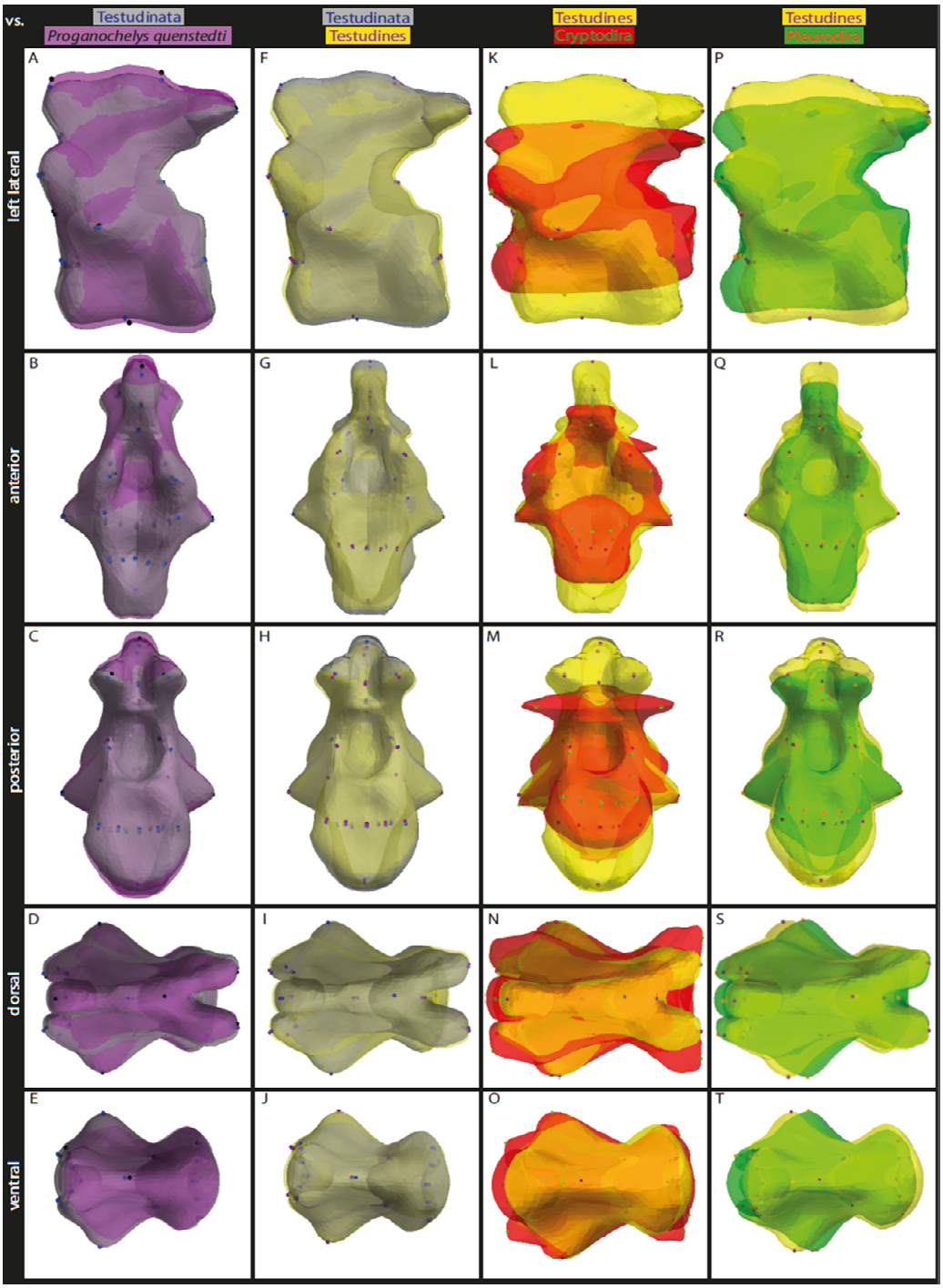


**Fig. 5.** Visualization of vertebral shape change through evolution. Cervical vertebra 2. All vertebrae brought to same scale. Color code (also see table head): purple with black landmarks (LM): *Proganochelys quenstedti*; gray with blue LM: Testudinata (node 2); yellow with purple LM: Testudines (node 5); red with green LM Cryptodira (node 7); green with orange LM: Pleurodira (node 34). For interactive animation compare to Supplementary Files 2, 5, 8, and 11.

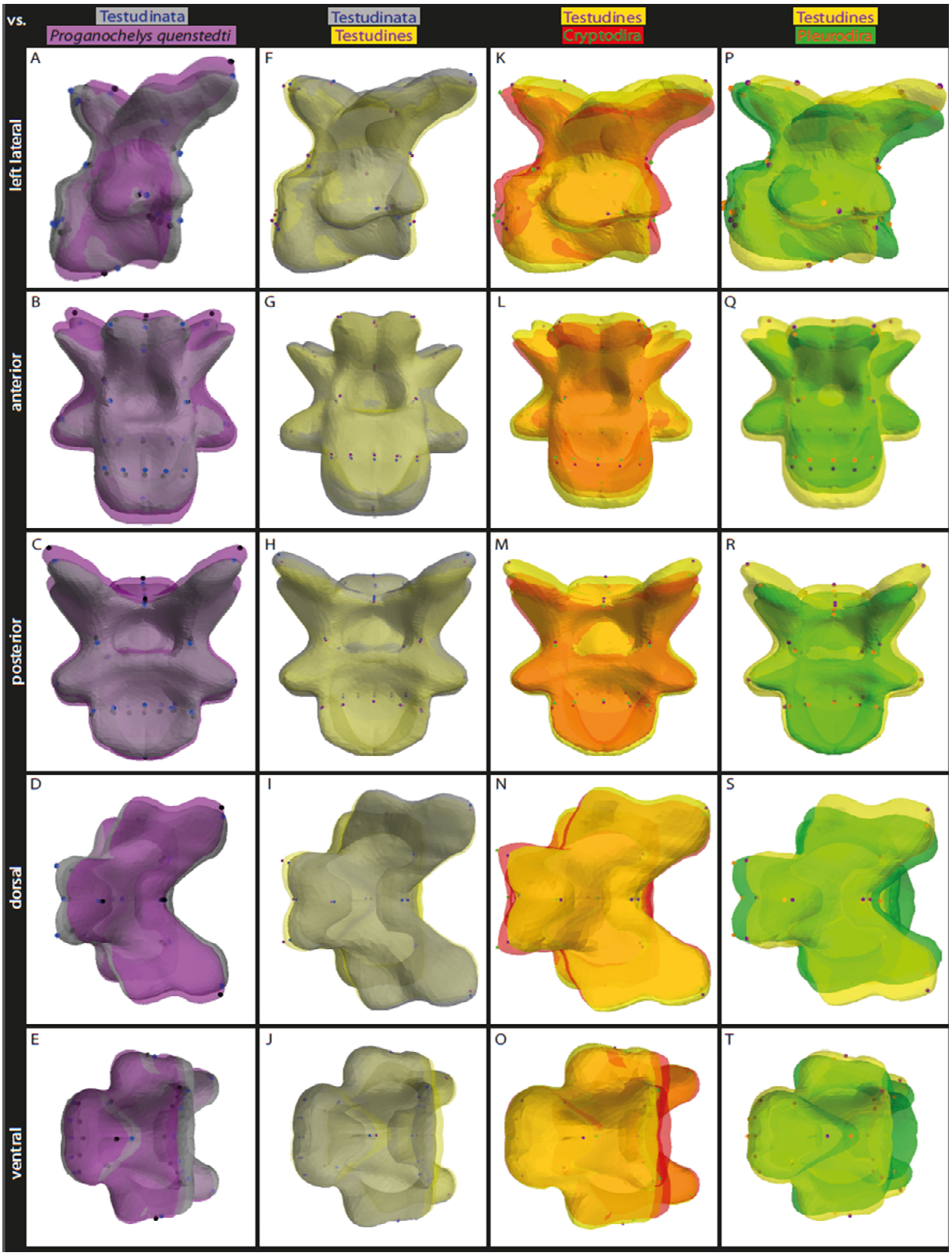


**Fig. 6.** Visualization of vertebral shape change through evolution. Cervical vertebra 5. All vertebrae brought to same scale. For color code see Fig. 5 and table head. For interactive animation compare to Supplementary Files 3, 6, 9, and 12.

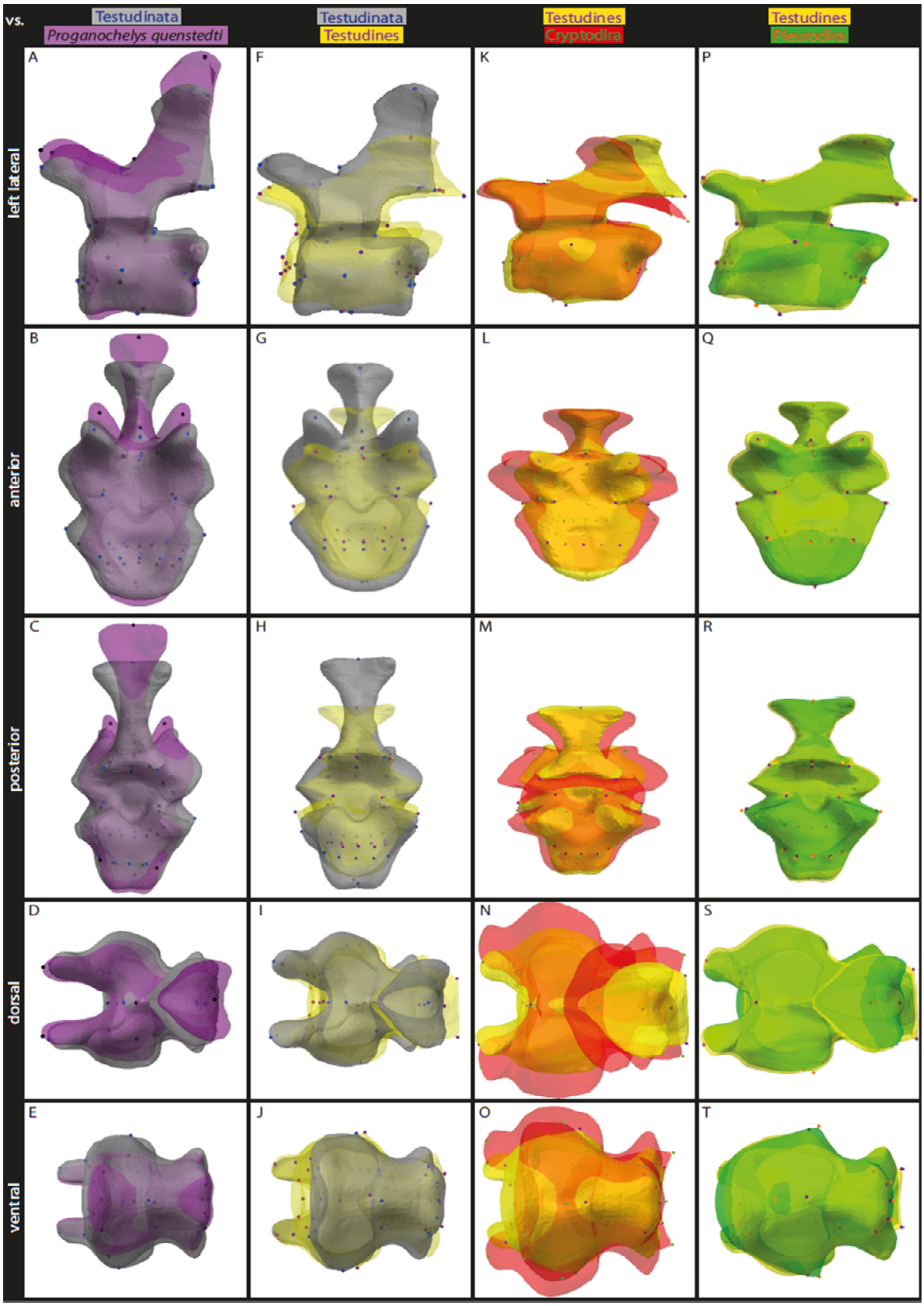


**Fig. 7.** Visualization of vertebral shape change through evolution. Cervical vertebra 8. All vertebrae brought to same scale. For color code see Fig. 5 and table head. For interactive animation compare to Supplementary Files 4, 7, 10, and 13.

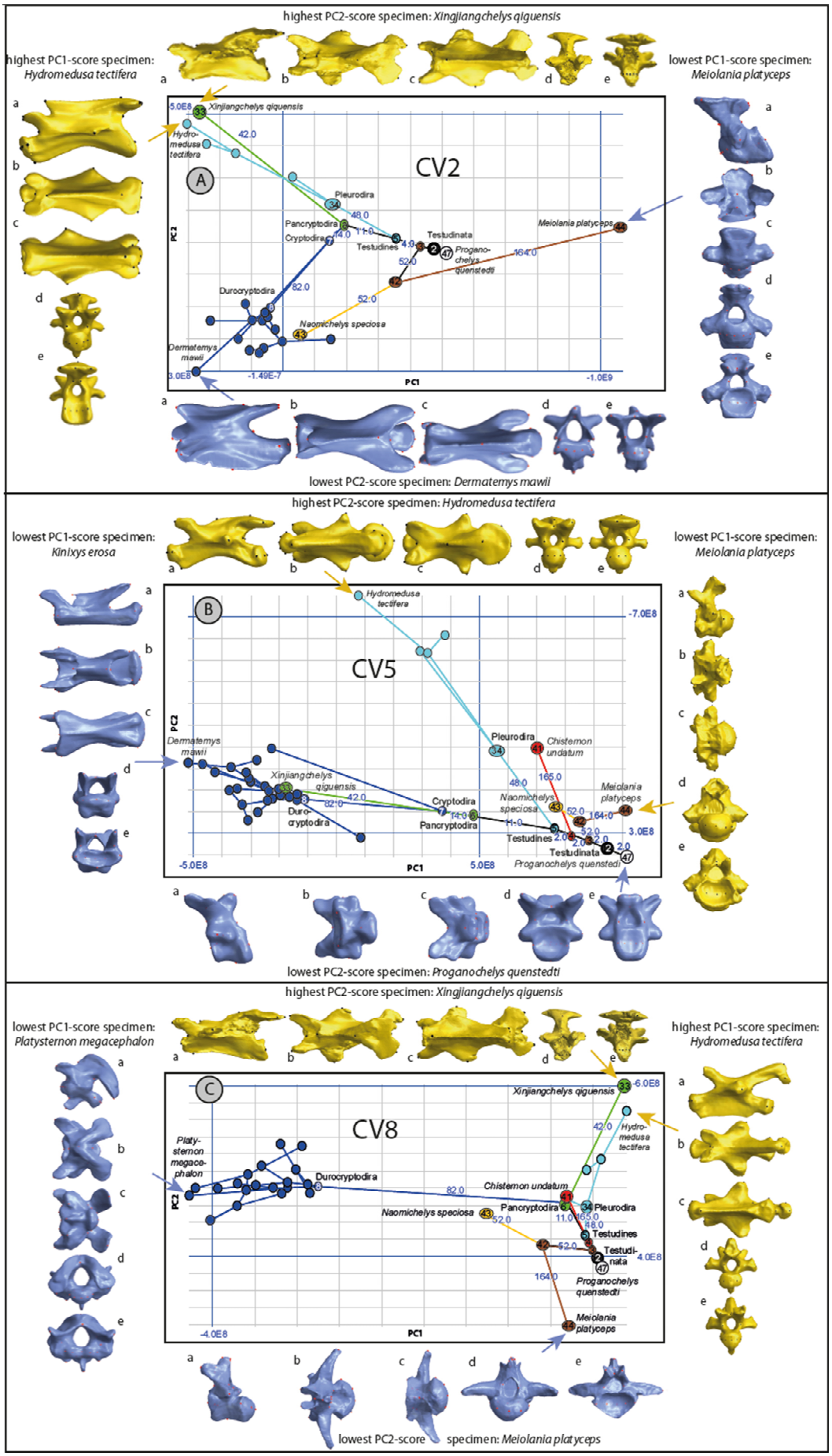

**Fig. 8.** Phylomorphospace-diagram of PC1 (vertical axes) / PC2 (horizontal axes) using the shapes of cervical vertebra (CV) 2 (A), CV5 (B), CV8 (C). Shape variance for the mean shapes of CV2: PC1 = 38.0%, PC2 = 21.3%; of CV5: PC1 = 49.4%, PC2 = 19.0%; and CV8: PC1 = 35.2%, PC2 = 19.0%. Blue numbers along the branches represent branch length. For colors, taxa, and node numbers compare to Fig. 4. For detailed diagrams of PC1/PC2 and for PC1/PC3 and PC2/PC3 see Figs. S7-9. Specimen illustrations of the highest and lowest PC1- and PC2-scores are provided in the Figure and correspond to the 3D-charts in Supplementary files 14-15.

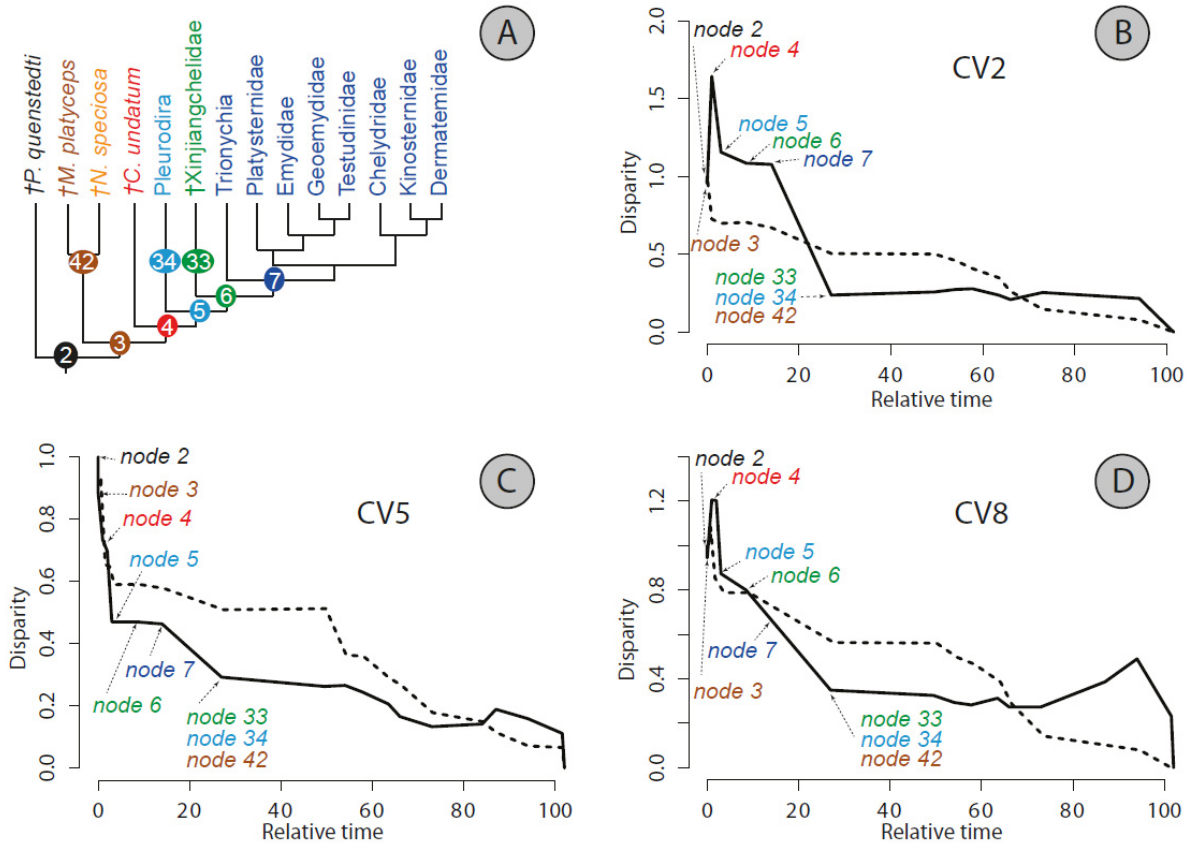


**Fig. 9.** Disparity across phylogeny (DAP) plot for vertebral shape (solid black line) data. A) Simplified topology (compare to Fig. 4). B) DAP chart for cervical vertebra (CV) 2, C) for CV5, D) for CV8. Disparity along the Y-axis is the average subclade disparity divided by total clade disparity calculated at each internal node. The dashed line represents evolution of the data under Brownian Motion (BM) simulations on the same phylogeny. Time values are relative time as per (Harmon, Schulte et al. 2003), whereby 0.0 represents the root and 1.0 represents the tip. 0% of relative time corresponds to 218 million years (my), the divergence time of Testudinata. 100% of relative time corresponds to recent time (0 my) (Fig. 4, Table S9). The most recent 10% of the plot can be omitted as it influences the effect of "tip overdispersion".

## Table Caption

**Table 1.** Results of Procrustes distance calculations for CV2, CV5 and CV8. Goodall's F-test values were bootstrapped (900 replicates) and values for 5% and 1% distributions are provided for comparison with the observed F-value. If the F value is greater than the value shown in the 5% column it is a significant result (shown in bold).

| | | | | | | Bootstrapped F | | | | |
|---|---|---|---|---|---|---|---|---|---|---|
| **Vertebra** | **Distance between** | | | **Proc dist** | **F** | **5%** | **1%** | **d.f. 1** | **d.f. 2** | ***P*** |
| CV2 | Testudinata | and | Pleurodira | 0,34241 | 2,1037 | 2,2072 | 2,9293 | 68 | 554 | 2.84-E06 |
| | | | Cryptodira | 0,35166 | **4,0731** | 3,2391 | 5,5023 | 68 | 554 | <1E-16 |
| | Testudines | and | Pleurodira | 0,30491 | 1,6682 | 2,194 | 3,1225 | 68 | 554 | 0,00115 |
| | | | Cryptodira | 0,31601 | **3,289** | 2,8958 | 4,4796 | 68 | 554 | 1,13E-14 |
| | Cryptodira | and | Pleurodira | 0,30509 | **7,7147** | 2,5211 | 4,8958 | 68 | 680 | <1E-16 |
| CV5 | Testudinata | and | Pleurodira | 0,45218 | **4,0249** | 3,1727 | 4,7062 | 68 | 884 | <1.0E-16 |
| | | | Cryptodira | 0,46566 | **7,3058** | 4,2964 | 9,3524 | 68 | 884 | <1.0E-16 |
| | Testudines | and | Pleurodira | 0,40589 | **3,2431** | 3,0065 | 4,5356 | 68 | 884 | 1,67E-15 |
| | | | Cryptodira | 0,42196 | **5,999** | 2,7262 | 6,5046 | 68 | 884 | <1.0E-16 |
| | Cryptodira | and | Pleurodira | 0,3756 | **12,8757** | 2,4144 | 4,1286 | 68 | 1020 | <1.0E-16 |
| CV8 | Testudinata | and | Pleurodira | 0,3628 | 1,8675 | 3,1551 | 5,0501 | 68 | 680 | 6,49E-05 |
| | | | Cryptodira | 0,402 | **4,0041** | 2,8698 | 4,6606 | 68 | 680 | <1.0E-16 |
| | Testudines | and | Pleurodira | 0,2477 | 0,8711 | 2,6613 | 5,8247 | 68 | 680 | 0,75903 |
| | | | Cryptodira | 0,32031 | **2,5338** | 2,4495 | 3,0481 | 68 | 680 | 1,73E-09 |
| | Cryptodira | and | Pleurodira | 0,45749 | **9,7147** | 2,7905 | 5,4351 | 68 | 748 | <1.0E-16 |